FFI RAPPORT

Gun barrel wear studies based on physical kinetics

FRØYLAND Øyvind, MOXNES John F.

FFI/RAPPORT-2005/03822

Gun barrel wear studies based on physical kinetics

FRØYLAND Øyvind, MOXNES John F.

FFI/RAPPORT-2005/03822

FORSVARETS FORSKNINGSINSTITUTT
Norwegian Defence Research Establishment
P O Box 25, NO-2027 Kjeller, Norway

FORSVARETS FORSKNINGSINSTITUTT (FFI)
Norwegian Defence Research Establishment

P O BOX 25
N0-2027 KJELLER, NORWAY

UNCLASSIFIED

SECURITY CLASSIFICATION OF THIS PAGE
(when data entered)

REPORT DOCUMENTATION PAGE

1) PUBL/REPORT NUMBER	2) SECURITY CLASSIFICATION	3) NUMBER OF PAGES
FFI/RAPPORT-2005/03822	UNCLASSIFIED	32
1a) PROJECT REFERENCE	**2a) DECLASSIFICATION/DOWNGRADING SCHEDULE**	
FFI-V/860/01	-	

4) TITLE

Gun barrel wear studies based on physical kinetics

5) NAMES OF AUTHOR(S) IN FULL (surname first)

FRØYLAND Øyvind, MOXNES John F.

6) DISTRIBUTION STATEMENT

Approved for public release. Distribution unlimited. (Offentlig tilgjengelig)

7) INDEXING TERMS

IN ENGLISH:	IN NORWEGIAN:
a) Oxidation	a) Oksidering
b) Ablation	b) Ablasjon
c) Gas erosion	c) Gasserosjon
d) Carbon dioxide	d) Karbondioksid
e) Water vapour	e) Vanndamp

THESAURUS REFERENCE:

8) ABSTRACT

In this article a study of the gun barrel wear mechanisms has been carried out. We construct a mathematical model based on the theory of ordinary differential equations. The model includes heat transfer and particle transfer into the gun barrel. The external parameters in the model are fitted to results from physical kinetics. Solving the differential equations give results for the temperature of the gun barrel along the gun barrel.

We find agreement with experimental results. The heat flux into the gun barrel due to convective flow is very dependent on the flow pattern inside the cartridge of the projectile.

9) DATE	AUTHORIZED BY	POSITION
	This page only	
2006-09-28	Bjarne Haugstad	Director of Research

ISBN 82-464-1033-4

UNCLASSIFIED

SECURITY CLASSIFICATION OF THIS PAGE
(when data entered)

CONTENTS

Page

Gun barrel wear studies based on physical kinetics

1 INTRODUCTION

Nammo Raufoss AS is the inventor of the Multipurpose (MP) ammunition concept. The MP technology was developed during the end of the 60s and the first series production started in the beginning of the 70s. Still the product is of great importance for the company's medium calibre division. Large volumes of ammunition are delivered for the armed forces around the world and in Norway.

Gun erosion has been known as an inevitable problem in use of current gun system, although extensive efforts have been paid to minimize it in the world. Gun erosion occurs as an increase in the bore diameter, allowing gas to escape past the projectile thus:

- reducing muzzle velocity
- reducing muzzle range
- reducing muzzle accuracy
- reducing penetration due to increased yaw
- increasing probability of premature during launching

The problems are rather common around the word and does not suggest any specific reason for doing research on gun barrel erosion in Norway, but using the MP ammunition gun barrel erosion has been seen to increase the probability of premature functioning of the round both in gun barrels and outside gun barrels. Also, the North Sea provides rough environments for gun barrels since salt or chloride decomposition into gun barrels is difficult to avoid. Salt or chloride decomposition on steel is known to enhance erosion significantly. A genuine understanding of the gun barrel erosion phenomenon could therefore be very profitable.

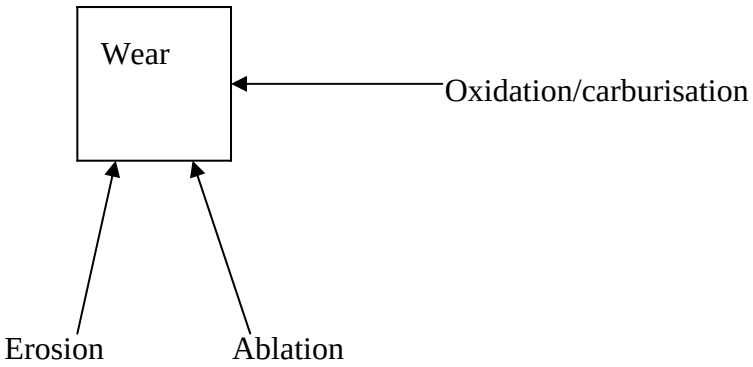

Figure 1: The different mechanisms affecting a gun barrel

Study of gun barrel erosion can conceptually be divided into different phenomena. First of all we believe that in order to achieve significant wear the following restrictions must be fulfilled:

- Increased temperature of the inner steel surface of the gun barrel. Increased temperature at the inside surface enhances mechanical wear, gun gases embrittlement and some chemical reaction processes.

- Enhanced brittleness of the inner steel surface of the gun barrel due to diffused gun powder gases. Gun gases can diffuse into steel and thereby restrict the dislocation motion in the steel. Enhanced brittleness is thereby achieved. Of special concern is the so-called hydrogen embrittlement. Hydrogen is a small molecule and diffuses easily into the steel lattice.
- Chemical reactions on the inner steel surface of the gun barrel. If the concentration of the diffused gases is large, chemical reactions such as oxidation/carburisation will lead to the oxide/carbide layer and increased brittleness of the steel.

Temperature

The temperature increases at the inside gun barrel surface due to heat convection of gun barrel gases, or due to friction between the projectile and the gun barrel. Further, its is important to separate between different fluid mechanics situations during erosion. If during burning of gunpowder quantities of gunpowder particles or gunpowder gasses are able to move between the gun barrel and the projectile, and finally ahead of the projectile, a large increase in the gun barrel radius has been observed pr shot. This fluid mechanic situation is called scoring, and is usually observed at the terminal stage of the gun barrel lifetime. It is believed that significant erosion due to scoring only appears at the terminal stage of the gun barrel lifetime. Probably one reason for this increase of the erosion is due to the very high velocity of the gunpowder gases when it moves between the projectile and gun barrel. Large velocity leads to large heat transfer into the gun barrel surface. Some minimal scoring is always observed during a shot since gases will always leak ahead of the projectile in the initial phase of the shot. This leak would increase the gun barrel wear. A second explanation for large heat transfer is that gunpowder particles can deadlock in the split between the gun barrel and the projectile while they are burning. Thereby facilitating a large local heat transfer to the gun barrel. It is important to be aware that scoring can dramatically increase the bore radius if the steering band or the jackets of projectiles are not correctly designed. Thus we believe that for a given gun power composition, scoring can be reduced by finding a fine tuned level of ductility, hardness and melting temperature of the steering bands or jackets of projectiles.

It is still important to remember that only gas leakage per se can reduce muzzle velocity, range and accuracy of a projectile. Also scoring will in general reduce the tight fit between the projectile and the gun barrel. Thus the internal relative motion of the projectiles during launching will increase. Increasing relative motion is well known to enhance the probability of premature during launching

Gun erosion due to gun powder gas or particles not leaking ahead of the projectile during launching is called gas erosion. It is believed that gun erosion is a necessary first condition for significant scoring. Thus, mathematical modelling and genuine hands-on knowledge of the physics and chemistry inherent in gas erosion will be one of the main objectives in this report.

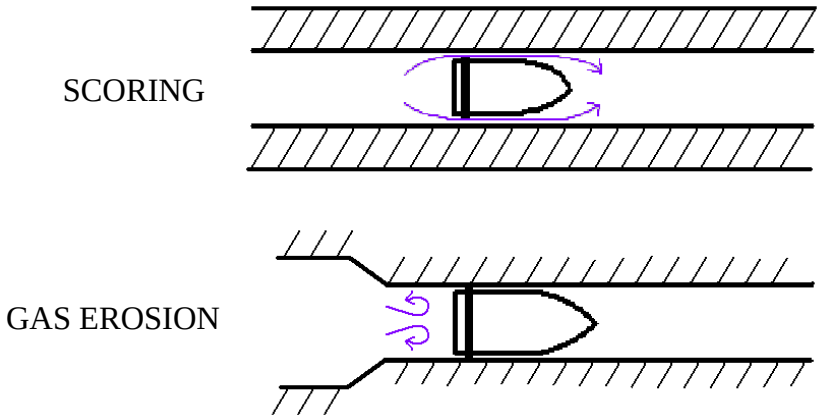

Figure 3: Scoring and gas erosion

The heat flux into (positive) into the gun barrel is due to four different mechanisms, a) the heat flux directly from the burning particles, which could have a higher temperature than the average gun powder gas temperature (flame temperature), b) the heat flux due to the hot gases with a temperature equal to the flame temperature, c) the heat flux due to the exothermal chemical reaction during the oxidation/carburisation process, and finally d) the heat flux due to mechanical friction between the projectile and the gun barrel. The heat loss is due to heat loss out of the surface layer into the surrounding area.

The situation in a) is very difficult to analyse and control since the main physics of this type of mechanism is difficult to establish. It is observed that when finely ground solid nitramines are used, the erosion is considerably less than when larger particles are used. One therefore believes that impingement of burning particles, which burn with higher flame temperature than the average flame temperature of the gas causes the increased erosion loss, although increasing wear due increased thermal stress also could be a significant factor.

The situation in b) is more easily analysed by using ordinary fluid mechanic heat transfer theory. The heat transfer is related to the so-called adiabatic wall temperature, which is the temperature close to the boundary layer. The adiabatic wall temperature is increasing with velocity of the gunpowder gases. Further the heat transfer coefficient is increasing with the density, velocity and conductivity of the gunpowder gas, but decreasing with the viscosity. The composition of different molecules in the gunpowder gas is therefore indirectly affecting the erosion due to the varying heat transfer and conductivity of the gas. Typically, hydrogen gas has high conductivity, and is accordingly believed to enlarge the heat transfer into the gun barrel. The heat flux due to chemical reactions is believed to be small for gunpowder. The heat flux due to mechanical friction can also be neglected.

Chemical reactions

The oxidation/carburisation and erosion phenomena both involve a host of different physical and chemical mechanisms and is therefore difficult to model mathematically from first principles.

The oxidation/carburisation is caused by the gun barrel gases, and/or by the oxygen of the incoming air reaching the inside surface of the barrel after a shot. Typically gun barrel gases consist of 45% CO, 20% H2O, 15% H2, 10% N2, and 10% CO2. The nitrogen is believed to

be non-reacting (inert). The gun barrel pressure is around 450MPa as a maximum, and the temperature is around 3000 K as a maximum. The oxidation/carburisation from the gun barrel gases is believed to happen when the projectile is in the barrel. The oxidation/carburisation is basically a transformation of the steel in the gun barrel surface into steel carbide (Fe3C), wustite (FeO), magnetite (Fe3O4), or hematite (Fe2O3), whereas the steel carbide and the wustite is believed to be the most important products. To simplify we can therefore say that the oxide/carbide layer consists of wustite and carbide.

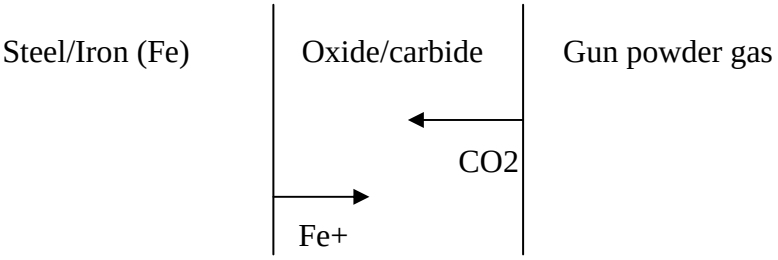

Figure 2: The oxide/carbide layer

The oxidation/carburisation will take place both at the outer surface (towards the gas) and at the inner surface (towards the steel). During outwards oxidation/carburisation iron ions effectively get free from the steel, diffuse outwards in the oxide/carbide layer and react finally with the adsorbed gunpowder gas at the inner surface of the gun barrel. During inward oxidation gas species diffuse inwards through the inner oxide/carbide layer and react finally with iron ions. Quit interestingly and important, the oxidation/carburisation as such, will decrease the inner radius of the gun barrel due to the rather low density of the oxide/carbide. The density is approximately 5500kg/m^3, but should have been 10000kg/m^3 to avoid this effect. Thus an inverse "erosion" mechanism is created.

The inner surface radius of the gun barrel increases due to wear and ablation. The wear and the ablation can be summarized as:

- Wear

1. the wear due to dry friction between the jacket of the projectile and the oxide/carbide layer
2. the wear due to failure (and off-tearing) of the oxide/carbide layer caused by stresses due to inhomogeneous thermal expansion of the layer and the steel
3. the wear due to detachment (and off-tearing) between the steel surface and the inner oxide/carbide layer facilitated by embrittlement of the steel
4. the wear due to failure (and off-tearing) of the oxide/carbide layer caused by stresses due to impingement of solid gun powder particles or due to friction with the jacked or due to pressure from hot gases.
5. the wear due to metal dusting of the steel
6. the wear due to a wipe off mechanism of melted oxide or carbide due to high velocity gases.

- Ablation

1. the ablation due to high temperature of the oxide/carbide layer caused by high temperature gun powder gases
2. the ablation due to high temperature of the oxide/carbide layer caused by high temperature gun powder particles burning close to the surface
3. the ablation due to high temperature of the oxide/carbide layer caused by the exothermial oxide/carbide reaction

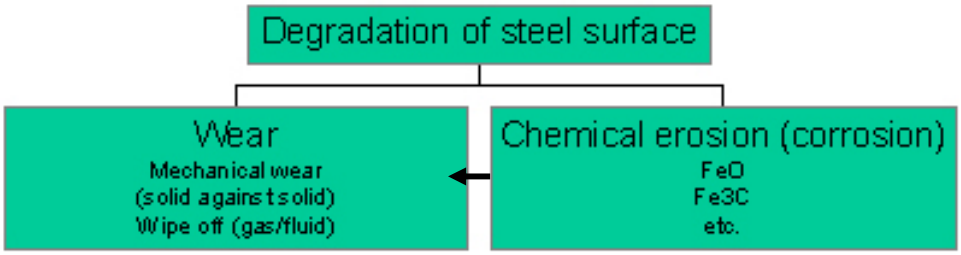

Figure 3: The degradation of a steel surface

We believe that the degradation of the steel surface due to ablation is small compared to the wear.

Our study starts with a theoretical study. Having accomplished this, we perform several studies to check the theory and the experiments. On doing the same for different types of gases, we identify the validity range of the analytical theory and finally provide simulations for gun barrel erosion.

2 MELT/WIPE-OFF AND EROSION OF HOT GASES.

The two main hypotheses on the mechanisms of wear are:

1) The wipe-off due to heating and melting of the surface. The heating is due to inert gases or chemical reactions on the surface. The melting temperatures of the reaction products are usually lower than for steel. Thus this wipe off is usually not significant.
2) The wipe off due to mechanical wear by high velocity gases or mechanically. The reaction products at the surface are of a brittle nature and are ripped off. Also increased brittleness of the steel is enhancing the wipe off.

The general mathematical solution of the problem must be based on the theory of partial differential equations. Our first approach is to model the main physical mechanism by formulating a theory based on ordinary equations. On doing this we hope to pinpoint the main physical mechanisms. Thereafter the fully partial differential equations can be constructed as the final equation set.

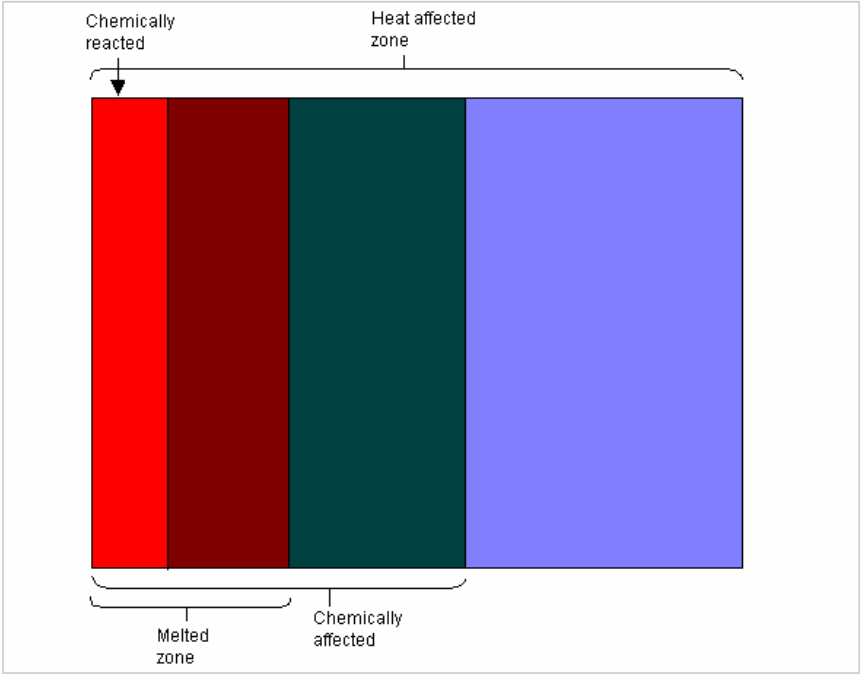

Figure 2.1: The different layers during wear

Consider a plane situation where the position is measured from the initial inner surface of the gun barrel. The following positions are important.

- r_H : The position of the zone affected by heat.
- r_G : The position of the zone affected by erosive gases
- r_M : The position of the melted zone
- r_R : The position of the chemical reacted zone
- r_S : The position of the inner surface of the gun barrel

The final objective is to calculate the position r_S which gives the degradation of the inner surface. Our study is somewhat pedagogical since we will start with the simplest case.

Heating of a solid surface

Consider a one-dimensional situation where surface where inert gas heats the surface. Let

- T_S : The temperature of the surface
- T : The temperature far away into the surface

Thus we provide the following mathematical model applying before the surface melt.

$$\underbrace{a\, l c_v \rho\, \Delta T_S}_{\text{Energy increase on the surface}} \overset{mod}{=} \underbrace{\dot{q}_i \Delta t\, a}_{\text{Influx of energy through the surface}} - \underbrace{\frac{k\left(T_S - T\right)a}{l}}_{\text{Energy loss from the surface into the solid}} \Delta t,\ when \quad \underbrace{T_S}_{\text{Surface temerature}} < \underbrace{T_M}_{\text{Melting temperature}}, (a)$$

$$\dot{r}_H \overset{mod}{=} \kappa / l, (b), \dot{r}_M \overset{mod}{=} 0, (c), \tag{2.1}$$

$$l \overset{def}{=} r_H - r_M = \kappa / l - \dot{r} = \kappa / l, \kappa \overset{def}{=} k /(c_v \rho), (d), r_M = 0$$

where k is the thermal conductivity at the surface, c_v is the heat capacity of the surface, ρ is the density, a is the area and l is length of the heat affected zone. T_M is the melting temperature. $\dot{q}_i$ is the heat flux per time unit and pr area unit. Equation (2.1a) say that the increase in internal energy of the surface of a layer of thickness l and area a during a time interval Δt equals the heat flux into the surface minus the heat loss due to heat conduction out of the surface into the material. This equation applies as long as the temperature of the surface is lower than the melting point T_m of the surface. Equation (2.1b) gives the relation for the length of the heat-affected zone. Equation (2.1) can be solved analytical for the situation where all parameters are constant, to read

$$\begin{aligned} &T_S(t) = T + \left(\frac{\dot{q}_i}{2^{1/2}(c_v \rho k)^{1/2}} \right) t^{1/2}, T_S < T_M \\ &T_S(t) = T_M \Rightarrow t = \underbrace{t_M}_{\text{Time to melt}} = \frac{2\left(T_M - T\right)^2 \left(c_v \rho k\right)}{\dot{q}_i{}^2} \end{aligned} \tag{2.2}$$

Thus the time t_M before melting increases inverse proportional with the heat flux raised to the power of 2. Also observe that the melting time is proportional with the thermal conductivity.

The melted surface

Assume that the melted layer is so thin that heat conduction is instantaneous in the melting zone. This can be achieved if the melted surface is removed, due to wipe off of gases or sliding surfaces, almost instantaneously as soon as it is formed. Thus the heat flux can be assumed to apply directly on the front of the melting surface close to the un-melted solid. This gives the following equation during melting

$$\underbrace{Q \rho\, a\, \dot{r}_M \Delta t}_{\text{Energy for melting}} \overset{mod}{=} \underbrace{\dot{q}_i a \Delta t}_{\text{Influx of energy through the surface}} - \underbrace{\frac{k\left(T_M - T\right)a}{l}}_{\text{Energy loss from the surface into the solid}} \Delta t,\ when\ T_S = T_M \tag{2.3}$$

Equation (2.3) says that the energy used for melting of an infinitesimal zone during a short time interval equals the energy fluxed into the surface minus the energy loss due to heat loss into the surface. This heat loss is proportional with the temperature difference and inversely proportional with a typical length scale of this difference.

Solving (2.3) for the stationary situation where the velocity of melting and the length of the heated zone relatively to the boundary are constant, gives directly for constant parameters

$$\dot{r}_M = \underbrace{\dot{r}_{M_{eq}}}_{\text{Steady state melting velocity}} = \frac{\dot{q}_i}{Q\rho} - \frac{k\left(T_M - T\right)}{l_{eq}Q\rho} = \frac{\dot{q}_i}{\left(Q\rho + \rho c_v\left(T_M - T\right)\right)} = \kappa / \left(l_{eq}\right), (a),$$
$$l = \underbrace{l_{eq}}_{\text{Steady state heat affected zone}} = \frac{\kappa\left(Q\rho + \rho c_v\left(T_M - T\right)\right)}{\dot{q}_i}, (b) \tag{2.4}$$

Equation (2.4) gives that the front velocity of the melting zone moves with a velocity proportional to the incoming heat flux. Observe the dependency of the heat capacity and the melting temperature which both tend to reduce the velocity of the melting surface for increasing values. Also note the dependency of the inner temperature T of the surface. Note that the heat conductivity does not influence the stationary velocity melting velocity. The reason is simply that although the size of the heated layer increases relatively to the boundary for increasing conductivity, the velocity of the surface stays constant since a decreased temperature gradient (due to increased conductivity) is compensated by increased conductivity over the gradient. This is easily seen from (2.4a) and (2.4b).

Combining (2.3) with (2.1) we reach the following more general model

$$\begin{aligned}
&T_S < T_M, \\
&\dot{T}_S(t) = \frac{\dot{q}_i}{lc_v\rho} - \frac{k\left(T_S - T\right)}{l^2 c_v \rho}, \dot{r}_M = 0, \dot{l} = \frac{\kappa}{l} - \dot{r}_M \\
&T_S = T_M, \\
&\dot{T}_S(t) = 0, \dot{r}_M = \frac{\dot{q}_i}{Q\rho} - \frac{k\left(T_M - T\right)}{lQ\rho}, \dot{l} = \frac{\kappa}{l} - \dot{r}_M
\end{aligned} \tag{2.5}$$

In order to close the solution set in (2.5) the heat flux into the surface must be modeled. This heat flux is established in the next section. For steel we first use the following material parameters to test the model:

$$\begin{aligned}
&T_M = 1800K, c_v = 500J/(kg\ K), \rho = 7900kg/m^3, k = 50W/\left(mK\right), \\
&Q = 2.7\,10^5 J/kg, \dot{q}_i = 10^9 W/m^2
\end{aligned} \tag{2.6}$$

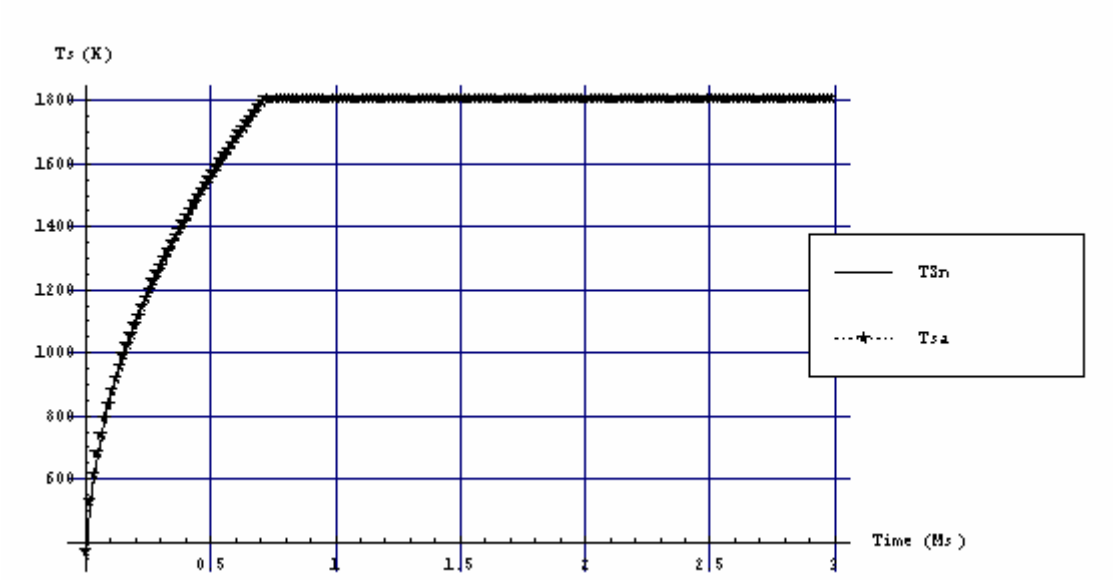

Figure 2.2: The surface temperature of the steel in Kelvin as a function of time in milliseconds using the parameters in (2.6). TSn is the numerical results and Tsa is the analytical result. The two results completely overlap.

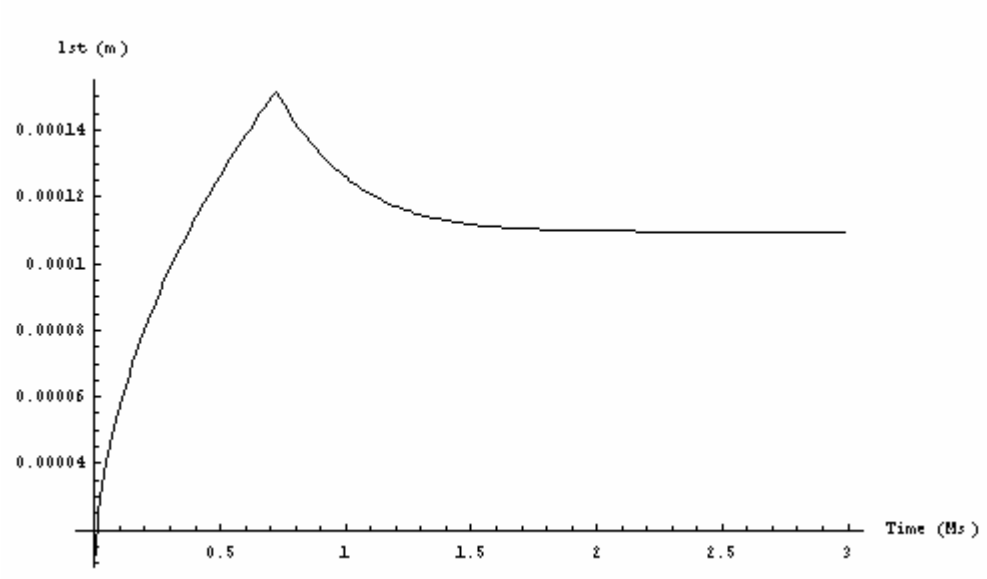

Figure 2.3: The length lst of the heat affected zone in meters as a function of time in milliseconds using parameters in (2.6)

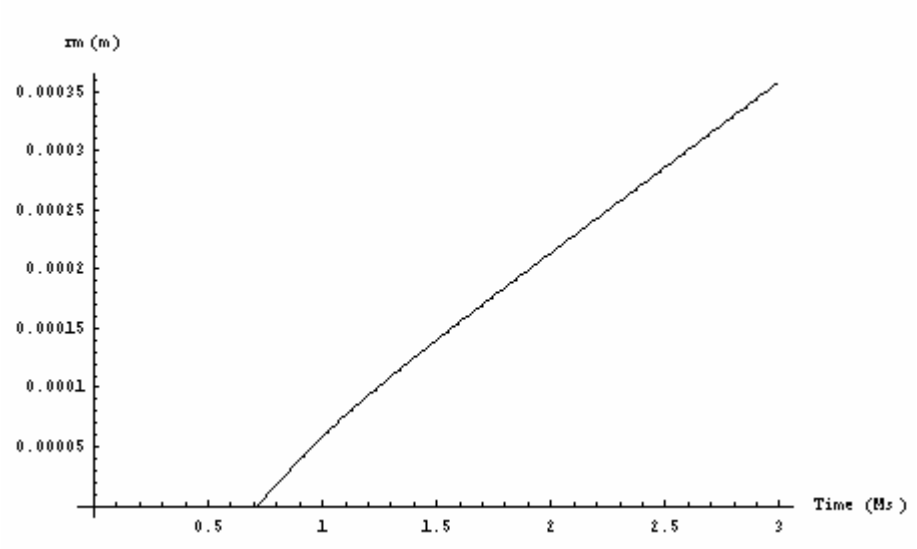

Figure 2.4: The length rm of the melted zone in meters as a function of time in milliseconds using the parameters in equation (2.6).

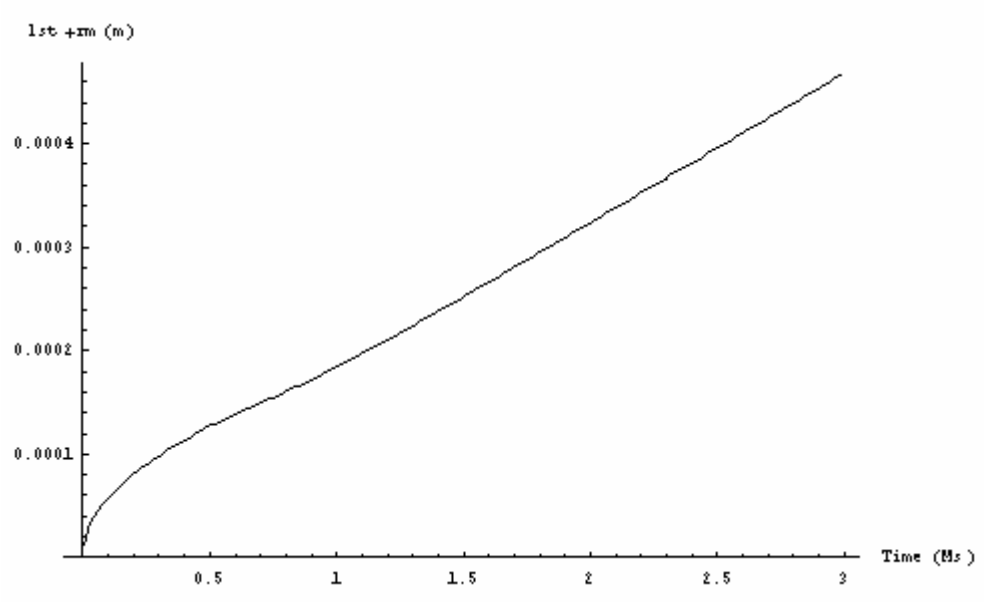

Figure 2.5: The length of the sum of the heat affected and melted zone in meters as a function of time in milliseconds using the parameters in equation (2.6).

Chemically reacted surface

We now turn to the chemical reaction mechanisms. Let

- C_S : The concentration of the gases at the surface
- C_R : The concentration when chemical reaction is finished
- C: The concentration far into the solid

We provide the following equation before chemicals reactions take place

$$C_S < C_R$$

$$\underbrace{a l_d \Delta C_S}_{\substack{Increase \\ in\ number\ of\ particles}} \overset{mod}{=} \underbrace{\dot{J} a \Delta t}_{Influx\ of\ particles} - \underbrace{\frac{D(C_S - C) a \Delta t}{l_d}}_{Outflux\ of\ particles}, \; \dot{l}_d \overset{mod}{=} D / l_d - \dot{r}_R, \dot{r}_R = 0 \tag{2.7}$$

This equation says that the increase in the number of particles in a volume $a l_d$ equals the flux of particles into the volume minus the loss of particles diffused out of the volume further into the surface. J is the flux of particles into the surface. D is the diffusion parameter, which depends on the temperature. The exact relation will be studied later. C is the concentration far into the solid. Observe that the length scale of the diffused layer is given by l_d, while the length scale of the heated layer was given by l. This equation applies as long as the concentration is lower than the reaction concentration C_R of the surface. Equation (2.7) can be solved analytical for the situation where all parameters are constant, to read

$$\begin{aligned} &C_s(t) = C + \left(\frac{\dot{J}}{2^{1/2} D^{1/2}} \right) t^{1/2}, C_s(t) < C_R, T_S < T_M \\ &C_s(t) = C_R \Rightarrow t = \underbrace{t_R}_{Time\ to\ react} = \frac{2(C_R - C)^2 D}{\dot{J}^2} \end{aligned} \tag{2.8}$$

Thus the time t_R to reaction increases inversely proportional with the particle flux raised to the power of 2. Also observe that the reaction time is proportional with the diffusivity.

Assume that after some time the concentration at the surface reaches higher values and chemical reactions take place. The concentration then level off. An oxide or carbide layer is created. Assume that the reacted layer is thin such that the particle flux is instantaneous in the reaction zone. Thus the particle flux can be assumed to apply directly on the front of the reacted surface in contact with the solid. Thereby increasing the position of the reacted zone, instead of increasing the concentration in the reacted zone. Thus we have

$$\begin{aligned} &C_S = C_R, \\ &a Q_d C_R \dot{r}_R \Delta t \overset{mod}{=} \dot{J} a \Delta t - \frac{D(C_R - C) a}{l_d} \Delta t \end{aligned} \tag{2.9}$$

where Q_d is a non dimensional factor which relates the thickness of the reaction layer for a given number of particles fluxed into the reaction layer. Equation (2.9) says that when the oxide or carbide front has moved a distance during a short time interval, this is related to the flux of particles into the surface minus the flux out of the surface into the solid.

The steady state solution is given by

$$\dot{r}_R = \underbrace{\dot{r}_{R_{eq}}}_{\text{Steady state reaction velocity}} = \frac{\dot{J}}{\left(C_R Q_d + \left(C_R - C\right)\right)},\ l_{d_{eq}} = \frac{D\left(Q_d C_R + \left(C_R - C\right)\right)}{\dot{J}} \tag{2.10}$$

Equation (2.9) and (2.10) give the following equation when the heat flux due to the chemical reaction is added to the heat flux

$$\begin{aligned}
&T_S < T_M,\\
&\dot{T}_S(t) = \frac{\dot{q}_i + H\left(\dot{J} - \frac{D\left(C_S - C\right)}{l_d}\right)}{l c_v \rho} - \frac{k\left(T_s - T\right)}{l^2 c_v \rho}, \dot{r}_M = 0, \dot{l} = \frac{\kappa}{l} - \dot{r}_M - \dot{r}_R, (a)\\
&T_s = T_m,\\
&\dot{T}_S(t) = 0, \dot{r}_M = \frac{\dot{q}_i + H\left(\dot{J} - \frac{D\left(C_S - C\right)}{l_d}\right)}{Q\rho} - \frac{k\left(T_m - T\right)}{lQ\rho}, \dot{l} = \frac{\kappa}{l} - \dot{r}_M - \dot{r}_R, (b)\\
&C_S < C_R,\\
&\dot{C}_S = \frac{\dot{J}}{l_d} - \frac{D\left(C_s - C\right)}{l_d^{\,2}}, \dot{r}_R = 0, \dot{l}_d = \frac{D}{l_d} - \dot{r}_R - \dot{r}_M, (c)\\
&C_S = C_R,\\
&\dot{r}_R = \frac{\dot{J}}{Q_d C_R} - \frac{D\left(C_R - C\right)}{l_d Q_d C_R}, \dot{l}_d = \frac{D}{l_d} - \dot{r}_R - \dot{r}_M, (c), (d)
\end{aligned} \tag{2.11}$$

where H is the heat of reaction pr particle. By comparing the relations in (2.11) with equation (2.5) we see that the reaction equations can established from the thermal equations by the substitution

$$\begin{aligned}
&\rho \to 1, c_v \to 1, T_s \to C_s, T_m \to C_R, Q \to C_R Q_d\\
&l \to l_d, \dot{q} \to \dot{J}, k \to D, \kappa \to D,
\end{aligned} \tag{2.12}$$

3 THE KINETIC PARAMETERS FOR THE GASES

During launching, different gunpowder gases interact with the gun barrel. The heat capacity, viscosity and conductivity are important for the heat transfer coefficient of the gunpowder gases. The diffusivity must be specified in order to establish the particle flux into the surface

The specific heat is most readily achieved, and different tabulated functions are found from the literature. Figure 3.1 gives the heat capacity as a function of the temperature for the different gases.

The molecules are attracted or repelled from each other according to molecular forces. Usually the Chapman-Enskog solution of the Boltzmann equation is employed together with

different approximation techniques. In order to apply the Chapman-Enskog solution one assume that

- The gas is sufficiently dilute for only binary collisions only to occur.
- The motion of the molecules during a collision can be described by classical mechanics
- The intermolecular forces depend only on the radial distance between the centres of mass of the molecules.
- Only elastic collisions occur

Our suggestion is that as long as the ideal gas law is applicable, the approximations can be used. The inter molecular Lennard-Jones 6-12 potential is assumed to be

$$V(r) = 4\varepsilon\left(\left(\frac{\sigma}{r}\right)^{12} - \left(\frac{\sigma}{r}\right)^{6}\right) \tag{3.1}$$

Various integral equations can then be found by using the Chapman-Enskog approach and numerical values are applicable.

Viscosity:

Assuming that (3.1) is valid gives that the viscosity can be written as

$$\eta = \frac{5}{16\pi}\frac{(\pi mT)^{1/2}}{\sigma^2\Omega_\eta}, \left(\eta = \frac{2}{3\pi}\frac{(\pi mT)^{1/2}}{\sigma^2}\right), \sigma \sim diameter \tag{3.2}$$

where m is the mass of the molecule and T is the temperature. Ω and σ can be found numerically and can be curve fitted from numerical solutions to give

$$\Omega_\eta(\varepsilon/k, T) = \frac{1.1614}{\left(\frac{kT}{\varepsilon}\right)^{0.149}} + 0.5248\, Exp\left(-0.773\left(\frac{kT}{\varepsilon}\right)\right) + 2.162\, Exp\left(-2.438\left(\frac{kT}{\varepsilon}\right)\right), \tag{3.3}$$

$$0.3 \le kT/\varepsilon \le 100$$

The different gases give the following relations

Gases	ε/k [K]	σ [Å]
Co	110	3.590
H2O	?	Polar
H2	38.0	2.915
N2	99.8	3.667
Co2	190	3.996

Table 4.1: Different parameters for gases used for viscosity calculations

It can be shown that for hard spheres $\Omega(T)$=1.

When gases are mixed the effective viscosity has to be calculated. The following relation is often used

$$\bar{\eta} = \sum_{i=1}^{N} \frac{\alpha_i \eta_i}{\sum_{j=1}^{N} \alpha_j \phi_{ij}}, \phi_{ij} = \left(\frac{m_j}{m_i} \right)^{1/2}, \qquad (3.4)$$

$$\bar{\eta} = \frac{\alpha_1 \eta_1}{\alpha_1 + \alpha_2 \phi_{12}} + \frac{\alpha_2 \eta_2}{\alpha_1 \phi_{21} + \alpha_2} = \frac{\alpha_1 \eta_1 m_1^{1/2}}{\alpha_1 m_1^{1/2} + \alpha_2 m_2^{1/2}} + \frac{\alpha_2 \eta_2 m_2^{1/2}}{\alpha_1 m_1^{1/2} + \alpha_2 m_2^{1/2}}$$

when we have N types of gases.

Conductivity:

Assuming that (4.1) is valid gives that the conductivity can be written as

$$\kappa = \frac{25}{32\pi} \frac{(\pi m T)^{1/2}}{\sigma^2 \Omega_k} \left(\frac{c_v}{m} \right), \left(\kappa = \frac{2}{3\pi} \frac{(\pi m T)^{1/2}}{\sigma^2} \left(\frac{c_v}{m} \right) \right), \sigma \sim diameter, \qquad (3.5)$$

$$\Omega_k \approx \Omega_\eta$$

where m is the mass of the molecule, T is the temperature and $c_v = (3/2)k$ is the heat capacity pr molecule due to translational motion. Using equation (3.2) for the viscosity gives that

$$\kappa = \eta \frac{5}{2} \left(\frac{c_v}{m} \right) = \eta \frac{15k}{4m} \qquad (3.6)$$

In binary collisions between polyatomic molecules, there may be interchanges between kinetic and internal energy. Such interchanges are not taken into account in the traditional Chapman-Enskog theory. It can therefore be anticipated that the Chapman-Enskog theory will not adequate describe the thermal conductivity for polyatomic gases.

To account for this the Eucken semi empirical approach is often used. One could from pure dimensional reasons write that

$$\frac{\kappa}{\eta \left(\frac{c_v}{m} \right)} = \left(\frac{5}{2} \right) \left(\frac{c_{tr}}{c_v} \right) + f_{in} \left(\frac{c_v - c_{tr}}{c_v} \right), c_{tr} = (3/2)k \qquad (3.7)$$

The first part corresponds to the translatoric part of the heat capacity, and the last term to internal energy. We observe that for a monoatomic gas we achieve the same results as before since $c_v - c_{tr}$ =0 where c_{tr} is the translatoric part of the heat capacity. The problem is then to find f_{in}. Eucken assumed that f_{in}=1, thus we achieve from (3.7) the final solution

$$\kappa = \eta\left(1+\frac{9/4}{c_v/k}\right)\left(\frac{c_v}{m}\right) = \frac{5}{16\pi}\frac{\left(\pi m T\right)^{1/2}}{\sigma^2\Omega_\eta}\left(1+\frac{9/4}{c_v/k}\right)\left(\frac{c_v}{m}\right) \tag{3.8}$$

The Prandtl number is defined by

$$Pr = \frac{\eta\left(c_p/m\right)}{\kappa} = \frac{c_p}{\left(c_v+9/4k\right)} = \frac{c_p}{\left(c_p+5/4k\right)} \tag{3.9}$$

When gases are mixed the effective conductivity has to be calculated. The same relation as in (3.4) is used, to read

$$\bar{\kappa} = \sum_{i=1}^{N}\frac{\alpha_i\kappa_i}{\sum_{j=1}^{N}\alpha_j\phi_{ij}}, \phi_{ij} = \left(\frac{m_j}{m_i}\right)^{1/2}, \tag{3.10}$$

Diffusivity

Both experiments and theory show that diffusion can result from pressure gradients, temperature gradients, external force fields and concentration gradients. Only concentration gradients will be discussed in this section since we believe that those are the most relevant for the gun barrel erosion problem. We assume that species A diffuses in a mixture of A and B due to a concentration gradient of A. This gives from the Chapman-Enskog theory that

$$\begin{aligned} D_{AB} &= \frac{3}{16}\frac{\left(4\pi k m_{AB}T\right)^{1/2}\rho_N}{\pi\sigma_{aB}{}^2\Omega_D m_{AB}}, \\ \Omega_D &\approx \Omega_\eta\left(\varepsilon_{AB}/k, T\right), \rho_N = \left(\frac{V}{N}\right), \\ \frac{1}{m_{AB}} &= \frac{1}{2}\left(\frac{1}{m_A}+\frac{1}{m_B}\right), \end{aligned} \tag{3.11}$$

where m_A and m_B is the molecular mass and species A and B, respectively. ρ_N =V/N is the total volume particle density. Further the following relations are assumed

$$\sigma_{AB} = \frac{\sigma_A+\sigma_B}{2}, \varepsilon_{AB} = \left(\varepsilon_A\varepsilon_B\right)^{1/2} \tag{3.12}$$

The diffusivity of A in a mixture of different gases is more difficult to calculate, and different approximation techniques are applied. The simplest relation is Blanc's law, which assume that the different species diffuse in a homogeneous mixture of the other species. This gives that the flux of particles is proportional with the concentration gradient with an effective diffusion coefficient of

$$\frac{1}{\bar{D}_i} = \frac{1}{\sum_{j=1\neq i}^{N} x_i / D_{ij}} \tag{3.13}$$

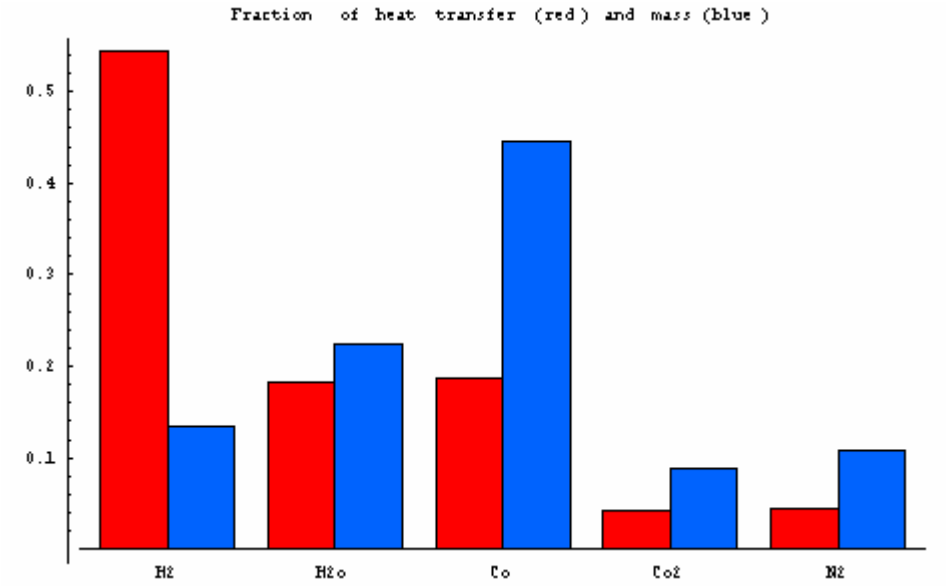

Figure 3.5: The fraction of heat transfer and mass transfer

We observe that hydrogen and the carbon dioxide contribute significantly to the heat transfer coefficient. The reason for the large hydrogen contributions is the high conductivity of hydrogen, and the reason for the high carbon monoxide contribution is the large mol fraction of carbon monoxide.

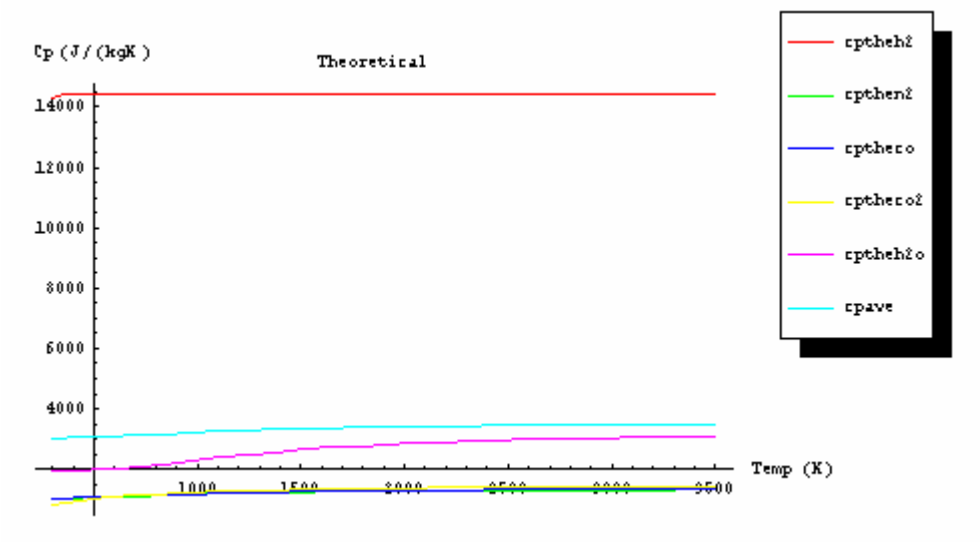

Figure 3.6: The heat capacity as a function of temperature.

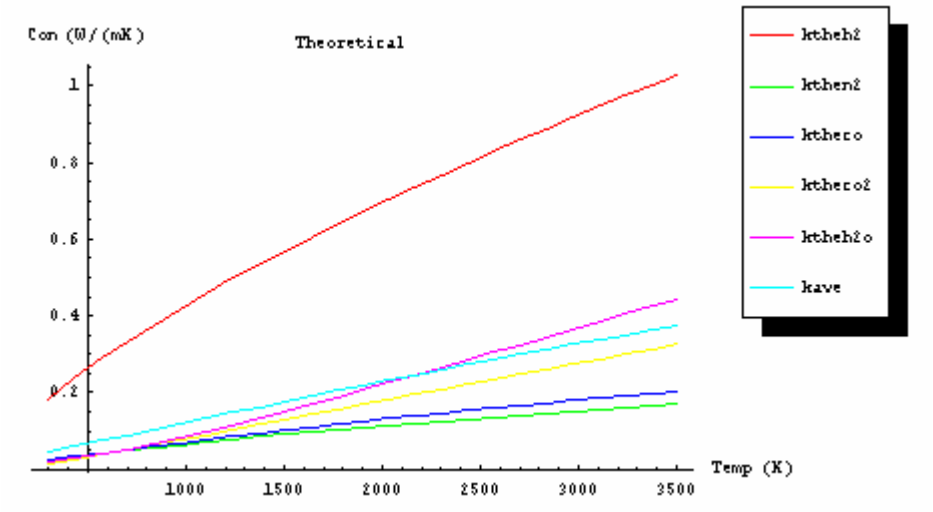

Figure 3.7: The conductivity as a function of temperature.

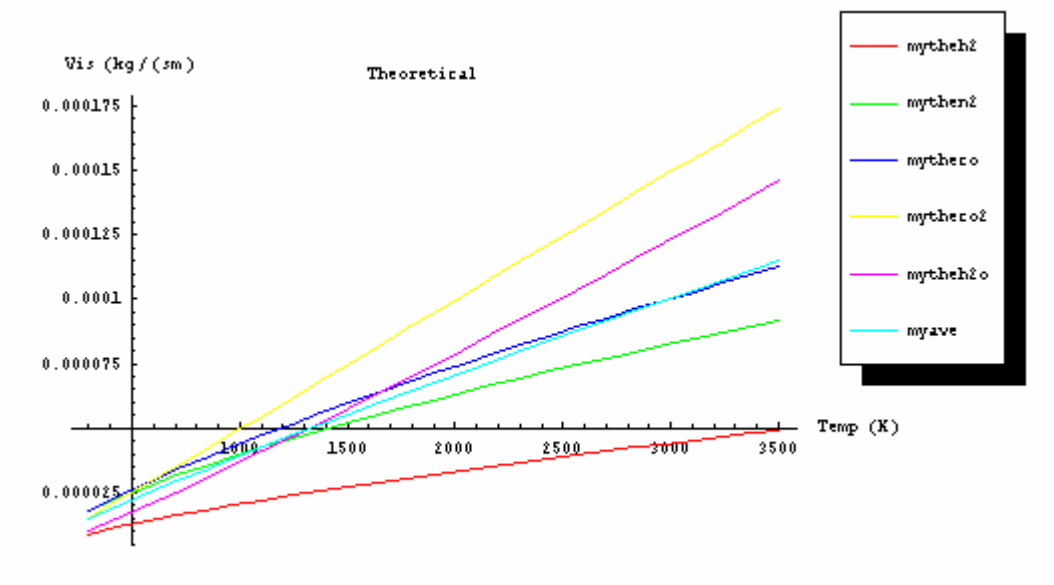

Figure 3.8: The viscosity as a function of temperature.

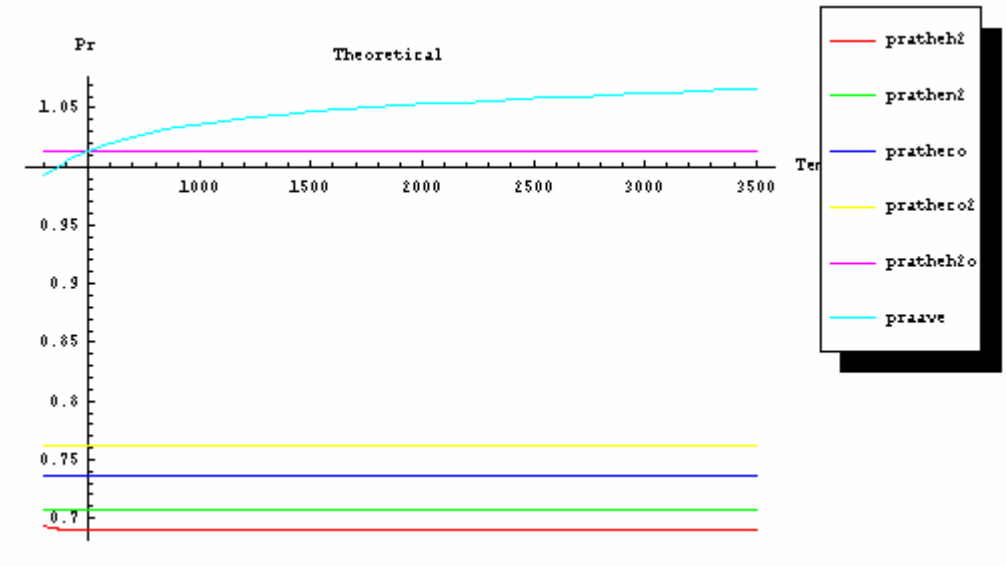

Figure 3.9: The Prandtl number as a function of temperature.

4 THE AVERAGE QUANTITIES

The temperature rise of the inside surface of the gun barrel is dependent on the position along the gun barrel. The main heat transfer is due to convection and not radiation.

We provide the following heat flux due to turbulent hot gases and friction

$$\dot{q}_i = \left(\left(T_{sol} - T_s \right) Nu^{av} \; k_g^{av} / L + \frac{f_f u}{a} \right), Nu^{av} = 0.037 \, (Pr^{av})^{1/3} (Re^{av})^{0.8}, \\ Pr^{av} = \frac{\mu_g^{av} c_g}{k_g^{av}}, Re^{av} = \frac{\rho v_p L}{\mu_g^{av}} \tag{4.1}$$

where Nu^{av} is called the average Nussel number and Re^{av} is the average Reynolds number and Pr^{av} is the average Prandtl number, k_g is the average thermal conductivity of the propellant gas, μ_g is average the viscosity, c_g is the average heat capacity during constant pressure. T_{sol} is "the solvability of the temperature" in the solid. L is a typical length scale of the flow. f_f is the friction force between the boundary and a moving surface. To calculate the average values we use the following algorithm

$$k_g^{av} = \sum n^i k_g^i / \left(\sum_i n^i \right), (a), \mu_g^{av} = \sum n^i \mu_g^i / \left(\sum_i n^i \right), (b), c_g^i = \sum n^i c_p^i / \left(\sum_i n^i \right), (c) \tag{4.2}$$

where n^i gives the number of mols of each species.

In order to close the solution set in (2.11) the particle flux into the surface must also be modeled. We provide the following particle flux due to turbulent gases

$$\dot{J} = \left(C_{sol} - C_s \right) Sh^{av} D_g / L, Sh^{av} = 0.037 \, (Pr^{av})^{1/3} (Re^{av})^{0.8} \\ Sc^{av} = \frac{\mu_g^{av}}{\rho D_g^{av}}, \tag{4.3}$$

C_{sol} is the solvability of the gases in the solid. D_g is the diffusivity of the propellant gas. Sh^{av} is the average Sherwood number and Sc^{av} is the average Schmidt number. Thus we use the same Reynolds number as during the thermal analysis.

Finally, the solvability is important to model. The following model is assumed

$$
\begin{aligned}
&T_{sol} = T_{aw}, (a) \\
&C_{sol}\left(C_{aw}\right) = \underbrace{\chi C_{aw}}_{\text{Physical solved}} + \underbrace{C_r\left(1 - Exp\left(-(\beta C_{aw})^2\right)\right)}_{\text{Chemical solved}}, (b) \\
&C_{aw} \approx C_g, T_{aw} \approx T_g, (c) \\
&\chi \sim 0.01, C_r \sim 5\,10^{28}/m^3, \beta \sim 4\,10^{-16} m^3,
\end{aligned}
\tag{4.4}
$$

The third law of thermodynamics stats that two objects in contact will ultimately reach the same temperature. This gives (4.4a) where T_{aw} is the adiabatic wall temperature, which is near the gas temperature. The solvability of the different gases is given by the sum of the physically solved material and the chemically solved material.

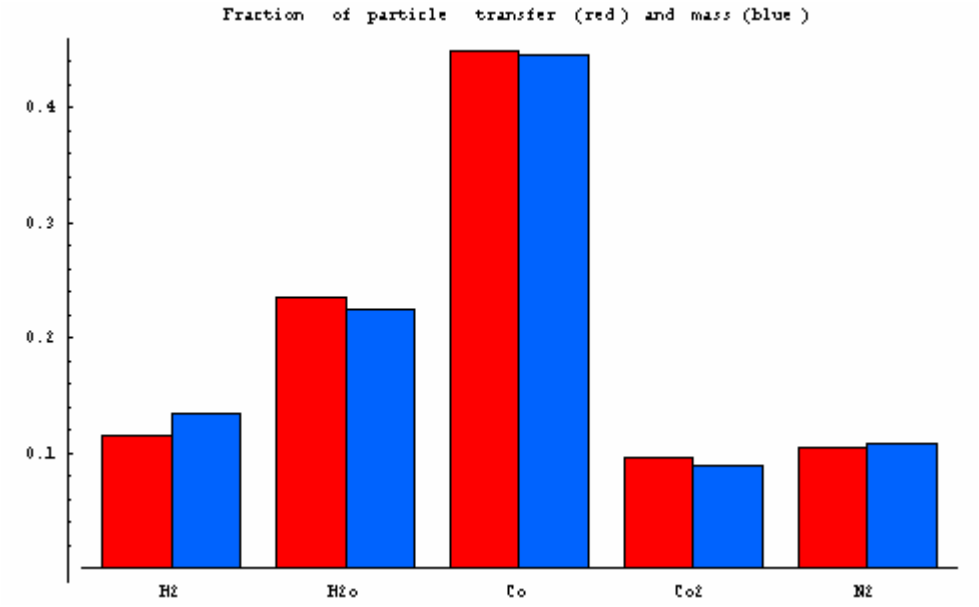

Figure 4.1: The relative particle and mass transfer as a function of the different molecules.

5 TEMPERATURE RESULTS FOR DIFFERENT GUN BARREL GASES

The temperature rise of the inside surface of the gun barrel is dependent of the axial position along the gun barrel. The heat transfer is due to convection and not radiation.

Bofors gun powder

Figure 5.1 show the heat transfer to the inner surface of the gun barrel as a function of the axial position along the gun barrel. It is assumed that the velocity of the gun barrel gases increases linearly from the base of the gun barrel (i.e. base of the cartridge) up to the projectile. For specific points along the axial direction, the heat transfer starts when the rear of the projectile reaches that position. The heat transfer function as a function of time is rather complex since

the density of the gases increases as function of time in the beginning due to the burning of the gun powder.

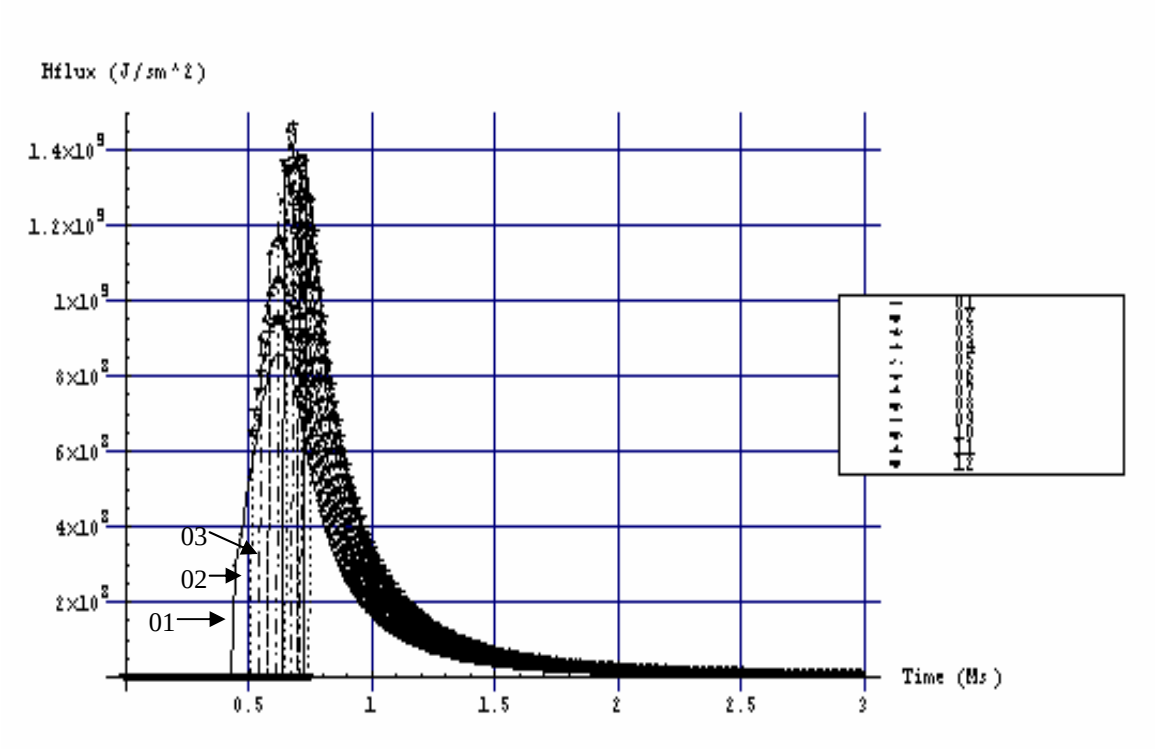

Figure 5.1: The heat transfer into the inside surface of the gun barrel for different positions along the gun barrel. Numbers give the distance in centimetres from the initial rear position of the projectile. The velocity of the gases is zero at the rear of the cartridge and is increasing linearly up to the projectile velocity at the rear of the projectile. Bofors gun powder.

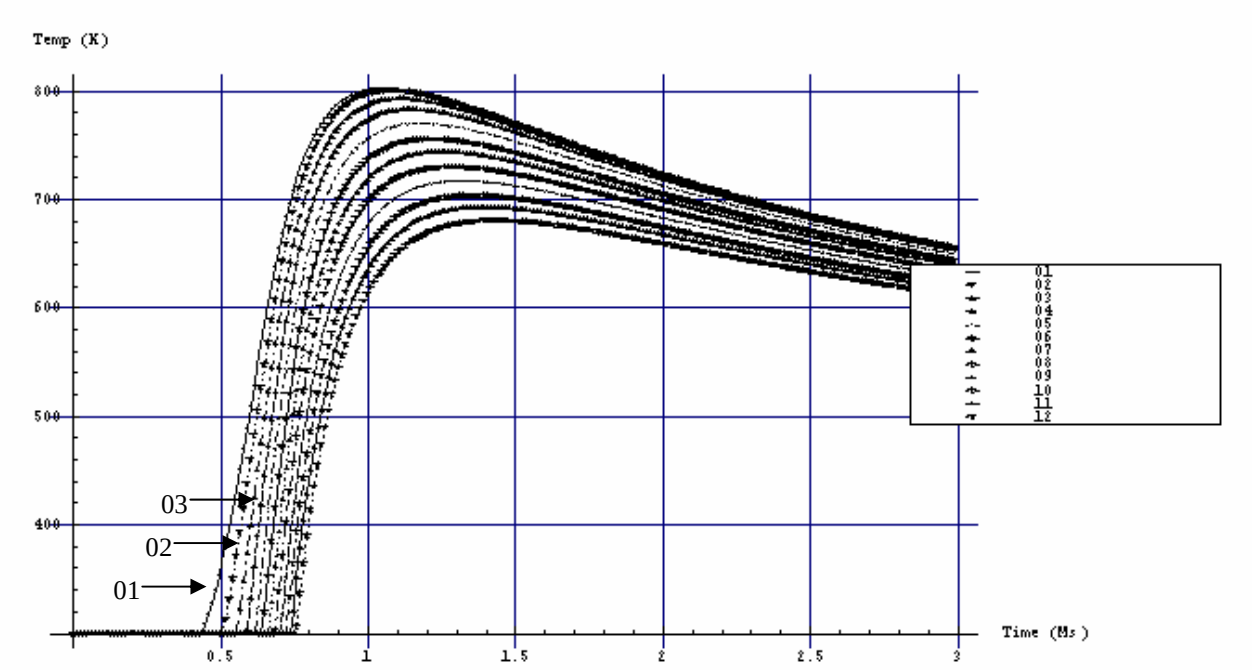

Figure 5.2: The temperature at the inside surface of the gun barrel for different axial positions along the gun barrel. Numbers give the distance in centimetres from the initial rear position of the projectile. The velocity of the gases is zero at the rear of the cartridge and is increasing linearly up to the projectile velocity at the rear of the projectile. Bofors gun powder.

Figure 5.1 shows that the spike of the heat flux reaches a maximum approximately 10 cm along the gun barrel. Figure 5.2 shows the temperature along the gun barrel is a maximum for the first curve, i.e. 1 cm from the initial rear position of the projectile. The reason for this difference is that the temperature is related to the total heat flux not only the spike of the heat flux.

According to the literature the following pure empirical formulae can be used for the inner bore surface temperature

$$T_{max} = T_i + \frac{\left(T_f - T_i\right)}{\sqrt{\frac{900}{C_m}}\left(1.7 + 670\, d^{2.22} / m^{0.86}\right)} \tag{5.1}$$

where T_{max} is the maximum temperature at the bore surface, T_i is the initial temperature of the bore surface, T_f is the adiabatic flame temperature, C_m is the initial velocity of the projectile, d is the inner bore diameter, and m is the charge mass. The temperatures are given in Kelvin and the other quantities are in SI units. Figure (5.3) shows the bore surface temperature as a function of the initial temperature. The melting temperature for FeO is 1660 K.

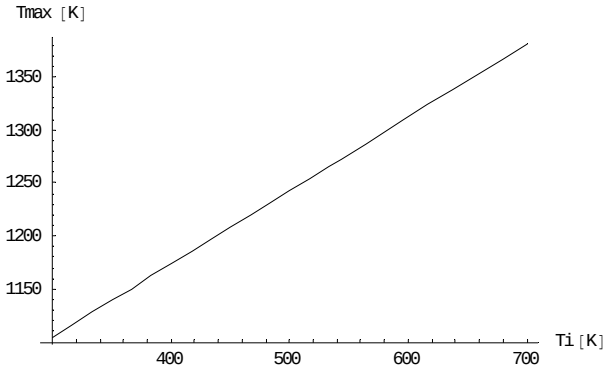

Figure 5.3: The maximum bore temperature as a function of the initial temperature of the bore. $C_m = 900m/s, m = 0.015kg, d = 0.0127m$, *(formula 5.1).*

We can compare the solution in Figure 5.3 with the spikes in Figure 5.2. We observe that our numerical results in Figure 5.2 are lower. We do not know the reason for this, but not including the effect of friction in the simulations could be the main reason.

One should notice that he temperature of the inside surface of the gun barrel is depending on the velocity profile of the gun barrel gases. When assuming that the velocity is zero for the initial position of the rear of the projectile and increasing linearly up to the projectile velocity, Figure 5.4 follows

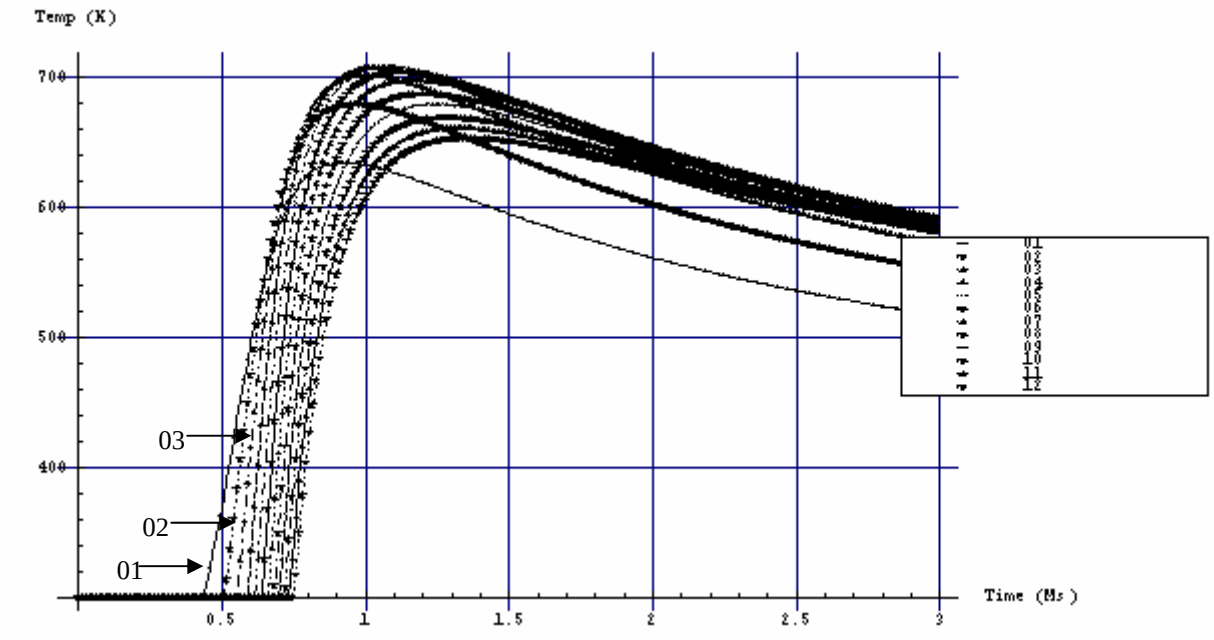

Figure 5.4: The temperature at the inside surface of the gun barrel for different axial positions along the gun barrel. Numbers give the distance in centimetres from the initial rear position of the projectile. The velocity of the gases is zero at the rear initial position of the projectile and

is increasing linearly up to the projectile velocity at the rear of the projectile. Bofors gun powder.

The temperature is lower than in Figure 5.2 and a maximum is reached approximately 3-4 cm from the initial rear position of projectile.

P B Clermont gun powder

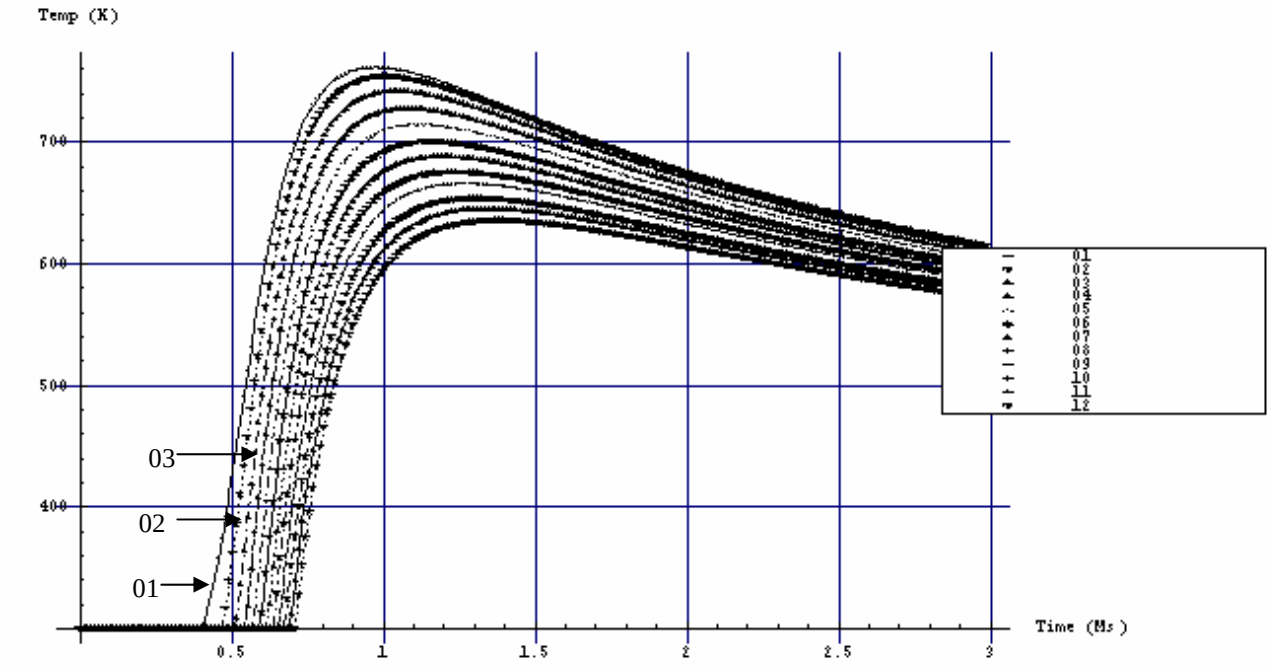

Figure 5.5: The temperature at the inside surface of the gun barrel for different axial positions along the gun barrel. Numbers give the distance in centimetres from the initial rear position of the projectile. The velocity of the gases is zero at the rear of the cartridge and is increasing linearly up to the projectile velocity at the rear of the projectile. P B Clermont gun powder.

Figure 5.5 can be compared with Figure 5.2. We observe that the P B Clermont gun powder gives smaller maximum temperature than the Bofors gun powder.

The erosion pr shot is given by the empirical formulae

$$erosion = A\,Exp[\,(T_{max} - 273)/69], A \in \left(10^{-7}\,\mu m, 4\,10^{-6}\,\mu m\right) \tag{5.2}$$

Thus the we achieve from Figure (5.2) and Figure (5.4) that

$$Exp[\,(T_{max} - 273)/69] = \begin{cases} 1162, when, T_{max} = 760K, Clearmont \\ 2075, when, T_{max} = 800K, Bofors \end{cases} \tag{5.3}$$

Thereby the Clermont gunpowder decreases the erosion with approximately 300%. The exit velocity is 50m/s higher for the P B Clermont than when using the Bofors gun powder.

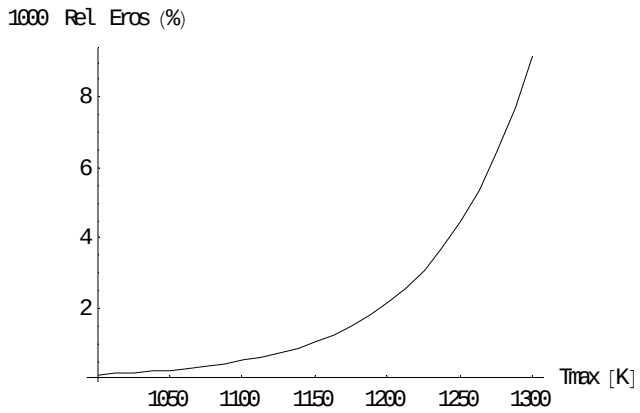

Figure 5.6: The erosion in percent of the bore radius pr 1000 shots as a function of bore surface temperature, $A = 2\,10^{-7}\,\mu m$.

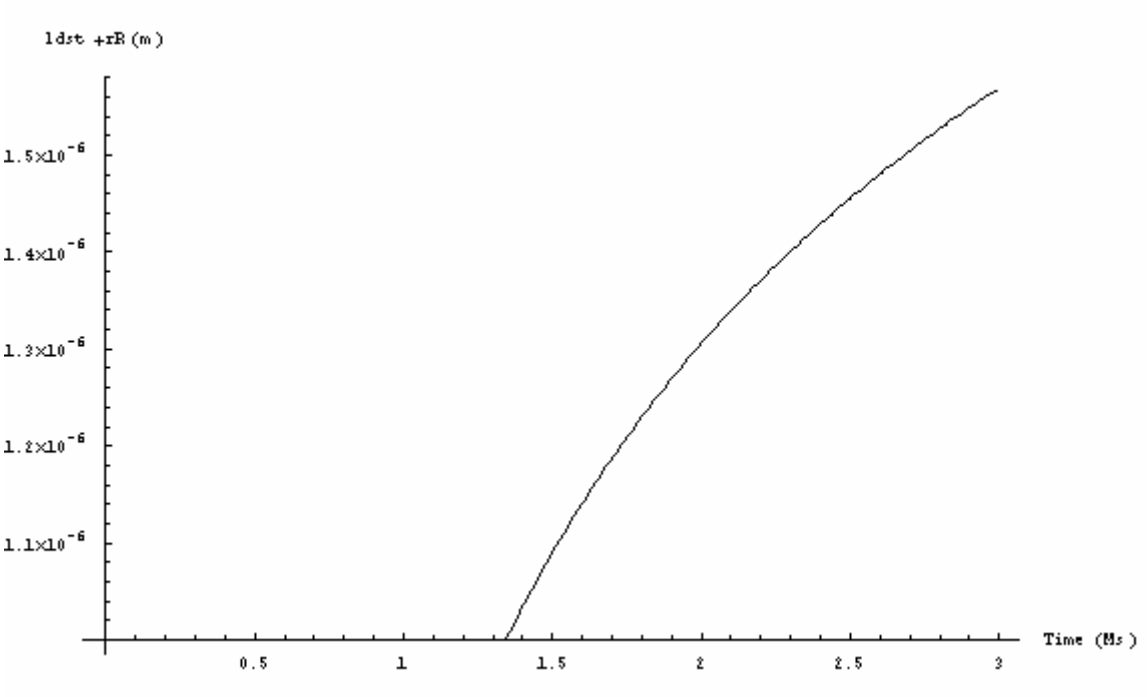

Figure 5.7: The length of the sum of the chemically reacted and chemically affected zone in meters as a function of time in milliseconds.

Figure 5.6 gives the erosion in percent of the bore radius as a function of the maximum temperature by using the formulae in equation (5.3). Figure 5.7 gives simulation results while

using equation (2.11). The erosion rate (assumed to be the chemically reacted zone) is approximately 0.5-micron pr shot.

An empirical formula is given by $erosion \sim m_c^{1.5} T_{max}{}^{7} v_0^{1.4} p_{max}^{5}$, where m_c is the loading mass, T_{max} is the maximum temperature of the gas, $v_0^{1.4}$ is the exit velocity of the projectile and p_{max} is the maximum pressure during a shot.

6 CONCLUSION/DISCUSSION

The temperature rise of the inside gun barrel is dependent of the position along the barrel. The heat transfer is mainly due to convection and not radiation. The heat transfer to the inside surface of the gun barrel is also dependent of the velocity profile of the gun barrel gases. We assumed that the velocity was linearly increasing from zero and reached the projectile velocity at the rear of the projectile. Assuming zero velocity at the initial rear position of the projectile gives lower heat transfer than when assuming zero velocity at the rear of the cartridge.

The erosion and the heat transfer for different gun barrel gases are found. The P B Clermont gun power gives the lowest convective heat transfer.

The temperature increase is smaller than found by an empirical formulae. We suggest that the reason for this is that the heat transfer due to frictional forces between the projectile and the gun barrel is not accounted for in our analysis.